Spectrochimica Acta Part A: Molecular and Biomolecular Spectroscopy 309 (2024) 123804

Contents lists available at ScienceDirect

Spectrochimica Acta Part A:
Molecular and Biomolecular Spectroscopy

journal homepage: www.journals.elsevier.com/spectrochimica-acta-part-a-molecular-and-biomolecular-spectroscopy

Spectroscopic probing of ultraviolet-induced degradation in elastomeric polyurea

Amritesh Kumar [a], David Pullman [b], George Youssef [a,*]

[a] Experimental Mechanics Laboratory, Mechanical Engineering Department, San Diego State University, 5500 Campanile Drive, San Diego, CA 92182, USA
[b] Department of Chemistry and Biochemistry, San Diego State University, 5500 Campanile Drive, San Diego, CA 92182, USA

HIGHLIGHTS

- Elucidated the photodegradation and photooxidation in elastomeric polyurea under ultraviolet.
- Studied conformational changes using spectroscopy techniques (THz-TDS, FTIR, EEM).
- Degree of H-bonding altered by exposing polyurea to ultraviolet.
- Ultraviolet radiation in ambient imparts fluorescence and self-absorption characteristics.
- Ultraviolet radiation in nitrogen atmosphere slows down the degradation of polyurea.

GRAPHICAL ABSTRACT

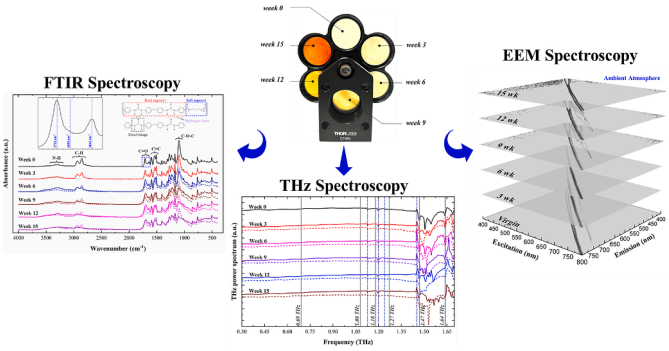

ARTICLE INFO

Keywords:
Terahertz spectroscopy
Polymer degradation
Ultraviolet radiation
Polyurea

ABSTRACT

Aromatic polyurea has garnered assiduous research due to its excellent impact, shock, abrasion, moisture, and chemical resistance properties. Polyurea can be used in protective coating and impact mitigation applications but is inevitably exposed to harsh deployment conditions such as extended ultraviolet (UV) radiation. Fourier Transform Infrared (FTIR) spectroscopy, Terahertz-time domain spectroscopy (THz-TDS), and Excitation-Emission Matrix spectroscopy (EEMS) deciphered the effects of UV radiation on radiated polyurea samples under ambient and nitrogen-rich conditions. Samples were radiated continuously for up to 15 weeks in increments of 3 weeks. Comprehensive FTIR analyses revealed a monotonic increase in disordered hydrogen bonding as a function of exposure duration in an ambient environment. Otherwise, marginal changes were observed in UV-radiated samples under nitrogen. The hydrogen bond length exhibited significant variations in the former compared to their nitrogen atmosphere counterparts. The results infer the nitrogen shielding effect, protecting polyurea from the photodegradation and photo-oxidation observed in samples radiated under the ambient atmosphere. THz-TDS spectra affirmed the FTIR results by probing changes in the complex refractive index. Terahertz spectral peaks associated with torsional vibrations of intermolecular hydrogen bonds in polyurea were notably correlated with increased exposure duration in the ambient atmosphere. Changes in the complex index as a function of exposure duration under nitrogen are minimal. The excitation-emission spectra of polyurea samples reveal a strong fluorescent behavior in 9-week and 12-week ambient-exposed polyurea due to cluster-triggered emission mechanisms. The results synthesized based on three different spectroscopy techniques

* Corresponding author.
E-mail address: gyoussef@sdsu.edu (G. Youssef).

https://doi.org/10.1016/j.saa.2023.123804
Received 31 October 2023; Received in revised form 19 December 2023; Accepted 21 December 2023
Available online 27 December 2023

paint a holistic portrait of the adverse effects of extended ultraviolet radiation of macromolecules deployed in harsh environmental conditions.

1. Introduction

Despite the emergence of aromatic polyurea in several impact mitigation applications and the sustained industrial and academic research over the past few decades, there are only a few sporadic investigations concerning its environmental stability and degradation [1–3]. Notably, formulating the alternative aliphatic polyurea was initially motivated by the susceptibility of the aromatic counterparts to ultraviolet (UV) radiation, suggesting the former is an ideal UV-stable top coat for the shock-tolerant protective coating of the latter [4–6]. The research vector on the effect of UV radiation on aromatic polyurea started only a few years ago but has recently evolved to elucidate the interrelationships between the exposure duration (*i.e.*, time in the artificial weathering enclosure) and environment (*e.g.*, oxygen-rich or -starved) and the degradation in the mechanical behavior [7–13]. At the onset, it is worth noting that polyurea encompasses a large set of chemical formulations that spans from linear to crosslinked structures, as recently summarized in [14]. The crosslinked version, with a specific cyanate and amine mixture, is ubiquitous in the impact mitigation community due to its phase-segregated microstructure, comprising hard and soft domains. Such dichotomy in the mechanical behavior within the domains stems from the thermodynamic incompatibility of the segments during polymerization [15], amplifying the impact and shock efficacy of this type of aromatic polyurea. Hence, the motivation leading to this research emphasizes the effect of extended exposure to ultraviolet radiation in artificial weathering conditions on the molecular structure of aromatic polyurea. Specifically, a focus is afforded to the evolution of the macromolecule as a function of ultraviolet radiation exposure duration using different spectroscopic techniques.

Aromatic polyurea is a thermoset elastomeric polymer with a broad range of protective applications in extreme conditions due to its impact and shock (as noted above), abrasion, moisture, and chemical resistance [1,16–18]. This aromatic macromolecule results from a step (addition) polymerization reaction of a diamine (*e.g.*, oligomeric diamine known commercially as Versalink® P1000 from Evonik) and diisocyanate (*e.g.*, polycarbodiimide-modified diphenylmethane diisocyanate denoted commercially as ISONATE 143L from Dow), resulting in semi-crystalline hard domains inter-dispersed within amorphous soft matrix [19]. The hard segments are interconnected by ordered (bidentate) and disordered (monodentate) hydrogen bonds from the amine and carbonyl groups of the urea linkages, giving rise to enhanced mechanical and physical properties. Since aromatic polyurea is used as a protective coating, extended exposure to ultraviolet radiation is imminent and could be detrimental in extended deployments. Hence, recent studies focused on the effect of ultraviolet radiation on the mechanical performance of aromatic polyurea without any modifying additives that may shift the absorption band (*e.g.*, pigments or colorants) or chemical modifiers (such as ultraviolet absorbers or antioxidants) [11,20]. While additives are known to mitigate the effect of a specific environmental or operating stimulus, they also have a pronounced influence on mechanical behavior [20–25]. In other words, additives and modifiers remedy a shortcoming while adversely altering the macromolecular structure and the mechanical performance concurrently. Imperatively, the latter is essential in the design of impact-tolerant and shock-absorbing protective structures, where the structural integrity of the macromolecule is paramount.

Youssef *et al.* reported the effect of extended ultraviolet radiation on the hyperelastic properties of polyurea, elucidating the photo-induced embrittlement by documenting *ca.* 24 % increase in the elastic modulus after 15 weeks of continuous artificial exposure [9]. Progressive morphological (surface roughness and superficial microcracking) and color evolutions also accompanied the hyperelastic mechanical changes as a function of the exposure duration, which Youssef and collaborators attributed to the interaction of oxygen and UV with the chromophore groups in the polyurea macromolecule [9]. Furthermore, they showed that the area under the stress–strain curve for unexposed and exposed samples remained unchanged while testing under the same quasi-static conditions [9]. In other words, Youssef *et al.* concluded that the hyperelastic behavior of aromatic polyurea remained unchanged even after 15 weeks of continuous exposure, promoting cascaded studies by the same group. It is worth noting that several studies on the effect of extended ultraviolet exposure on the response of aliphatic and aromatic polyurea were recently compiled in [26]. The primary conclusion from the latter summary is the confirmation of aliphatic polyurea to ultraviolet radiation, documenting potential for future impact mitigation applications by reinforcing with multi-walled carbon nanotubes, graphene, and other additives [27–29]. Nonetheless, aromatic polyurea has already been integrated into several industrial applications, including protective coatings in civilian and military applications such as commercial flooring, roof coatings, vibration reduction, impact and shock resilience armor, and corrosion-resistant marine applications. Owing to the current technological prevalence of aromatic polyurea, this research augments the existing knowledge on their long-term performance using novel spectroscopic measurements since this material class is foreseen in future applications in deployment environments.

In addition, other studies explored the effect of extended ultraviolet radiation on the mechanical behavior of aromatic polyurea, including acoustic, dynamic, thermal, and microstructural. Wye Ng *et al.* recently collated the primary results from experimental investigations on the effect of ultraviolet radiation on polyurea, summarizing the changes in the physical, morphological, mechanical, and chemical properties [7,8,10,11,30]. Youssef *et al.*, Shaik *et al.*, and Blourchian *et al.* reported the physical and morphological changes in aromatic polyurea sheets up to 15 weeks of continuous exposure in artificial weathering conditions at irradiated energy of $\sim$ 13.7 J/cm^2/h for the combined UV-A and UV-B radiation, corresponding to an accelerated weathering factor of 4.28 [7]. Youssef *et al.* observed that the original transparent yellow color of as-cast polyurea evolved to light tan after only three weeks of continuous ultraviolet exposure, with noted progressive darkening thereafter [9]. Youssef *et al.* postulated that the UV-induced discoloration (and formation of accompanying surface microcracks) is based on the interaction of oxygen, ultraviolet, and chromophoric groups in polyurea [10].

Shaik *et al.* focused on the mechanics of UV-induced microcracks, where the average crack opening monotonically increased as the exposure duration elapsed due to surface shrinkage associated with hard segment agglomeration [8]. Shaik *et al.* further concluded that a reduction in the local modulus suggests a potential mechanism for forming cracks due to the stress mismatch between the brittle surface and the compliant core [8]. Blourchian *et al.* found that extended exposure to UV radiation correlated with the hard domains, where the hard segment distribution increased from 66 % in the virgin sample to 75 % after 1.5 weeks of exposure [7]. Blourchian *et al.* also noted that the degradation depth ranged between 20 and 30 μm below the surface, leaving the core of the sample unchanged [7]. Finally, Che *et al.* studied the effect of marine conditions, including ultraviolet radiation, on the chemical structure of polyurea (consisting of diphenylmethane-4,4′diisocyanat, a polyether polyol, a terminal amino polyether, and an amine chain extender) using analytical techniques, including Fourier transform infrared (FTIR) and X-ray spectroscopies [13]. As mentioned above, the hard domains within aromatic polyurea give rise to monodentate and bidentate hydrogen bonding [13,14,31], corresponding to 1722 cm^{-1}, 1711 cm^{-1}, and 3340 cm^{-1} peaks detectable by FTIR based

on spectral peaks associated with the amine and carbonyl groups [13,32]. Che *et al.* reported (1) a decrease in peak intensities for ether and amide groups in the soft and hard segments, respectively, (2) changes in ordered and disordered hydrogen-bonded carbonyl group, and (3) peak broadening in peaks associated with hydrogen bonded amine [13]. Since Che *et al.* performed chemical analysis after exposing polyurea to marine conditions, including ultraviolet, one research question stands: *What are the effects of ultraviolet-only and oxygen-content on the chemical structure of aromatic polyurea?*

This research aims to elucidate the macromolecular conformational changes in aromatic polyurea after extended exposure to ultraviolet radiation in ambient conditions and nitrogen atmosphere using several spectroscopy techniques. In addition to probing virgin and irradiated samples with FTIR, a novel approach is introduced using terahertz time-domain spectroscopy configured in the transmission mode. The rationale for using THz-TDS stems from polymer transparencies to the electromagnetic spectrum within this range (<100 cm^{-1}) as well as the nondestructive and noninvasive nature of terahertz waves. Polyurea samples were exposed to ultraviolet radiation for extended periods of up to 15 weeks in ambient and oxygen-starved (nitrogen-rich) conditions at ambient temperatures. Therefore, the novelty of this research is twofold. First is utilizing a nondestructive yet penetrative spectroscopy to elucidate the damaging effects of ultraviolet on polymers. Second is the concurrent delineation between the effects of oxygen-rich and oxygen-starved environments on photodegradation.

2. Materials and methods

2.1. Samples preparation and exposure

Polyurea samples were prepared using step polymerization by thoroughly mixing oligomeric diamine (Evonik, Versalink P-1000) and diphenylmethane diisocyanate prepolymer (Dow, Isonate 143-L) at a 4:1 wt ratio, respectively. The resulting aromatic polyurea is a byproduct of the diamine extenders that impart high flexibility and initiate an exothermic reaction with the diisocyanate, yielding the segmented microstructure of hard and soft domains. The aromatic polyurea used in this study is a thermoset elastomer exhibiting high crosslinking from hydrogen bonding at the amine and carbonyl groups (*i.e.*, urea bonds). The mixture was poured into a $\sim 0.7 \pm 0.1$ mm deep aluminum mold from a height of approximately 1 m to facilitate the escape of entrapped air bubbles in the prepared mixture. The aluminum mold was coated with a non-sticky Teflon spray, circumventing the adhesion of the polyurea to the mold walls and promoting easy removal without compromising the surface texture of the prepared samples. The cast polyurea sheets were in ambient conditions for 24 h, then cured in a vacuum oven at 80 °C for an additional 24 h. Fig. 1 summerizes the sample preperation steps and the weathering process discussed next.

Circular disc samples, with 25.4 ± 1.2 mm diameter, were extracted from the cured polyurea sheet using a circular hammer-driven punch. The disc samples were randomly segregated into 11 groups, each comprised of three discs. One group was kept unexposed to UV radiation and treated as 'control' virgin samples. Five groups were artificially weathered simultaneously under ambient conditions. The samples were gently cleaned using isopropyl alcohol and deionized water to remove organic or particle contaminants. The UV radiation enclosure consisted of a light box (DoctorUV: DDU2024) fitted with four UV bulbs: two Philips TLK40W/03 bulbs emit UV radiation in the range of 300 to 460 nm with a peak wavelength of 360 nm, whereas the other two Philips TLK40W/05 bulbs emit radiation in the range of 380 to 480 nm with a peak of 420 nm. The inner surface of the chamber has been lined with mirror-finished stainless-steel sheets to maximize the UV radiation dosage during exposure. The samples were elevated from the bottom of the exposure (lined mirror-finished stainless steel) using a UV-transparent acrylic to ensure homogenous exposure. Notably, the enclosure was unsealed (*i.e.*, oxygen levels are comparable to atmospheric concentrations), indicating that the exposure was done under laboratory ambient conditions.

The UV system emitted 5122 mJ/cm^2 per hour and 8553 mJ/cm^2 per hour of UV-A and UV-B radiations, respectively, amounting to *ca.* 7200 h of natural weathering [11]. The UV flux was measured using a radiometer (EIT instrument Powerpuck II). The first set of samples was withdrawn from the chamber after three weeks based on the first observable color change in polyurea [11]. The remaining sets were removed sequentially at a three-week interval until the final set was pulled out after 15 weeks of continuous exposure. The final five groups of samples endured the same sequential levels of ultraviolet exposure duration and dosage as discussed above but in a custom-built sealed enclosure purged for a few hours with nitrogen before the experiment commenced. This enclosure was also lined up with the same mirror-finished stainless steel to homogenize the ultraviolet radiation dose on the sample surfaces. The purging step was necessary to evacuate the enclosure from ambient oxygen and moisture. An N_2 generator (Parker Domnick Hunter) maintained the nitrogen flow throughout the exposure duration. The sample cleaning, exposure, and extraction steps remained faithful to those discussed above. All the spectroscopic measurements reported herein were conducted at a constant room temperature of 22 °C. Furthermore, Whitten *et al.* previously discussed the engineering controls and measurements used in maintaining and monitoring the isothermal conditions during the exposure process [9,10].

2.2. Spectroscopic measurements

A broad range of spectroscopic measurements were utilized in this study, given the emphasis on elucidating the effect of extended ultraviolet radiation on the conformation of aromatic polyurea. Specifically, virgin, exposed under ambient atmosphere, and irradiated under N_2 atmosphere polyurea samples were characterized using (1) Fourier Transform Infrared (FTIR), (2) Terahertz Time-domain (THz-TDS), and (3) Excitation Emission Matrix (EEM) spectroscopies. It is worth noting that Raman spectroscopy measurements were initially pursued but quickly abandoned due to the photo-bleaching effects from the auto-fluorescence effect from the UV-degraded sampled, saturating the detector and deeming the data futile.

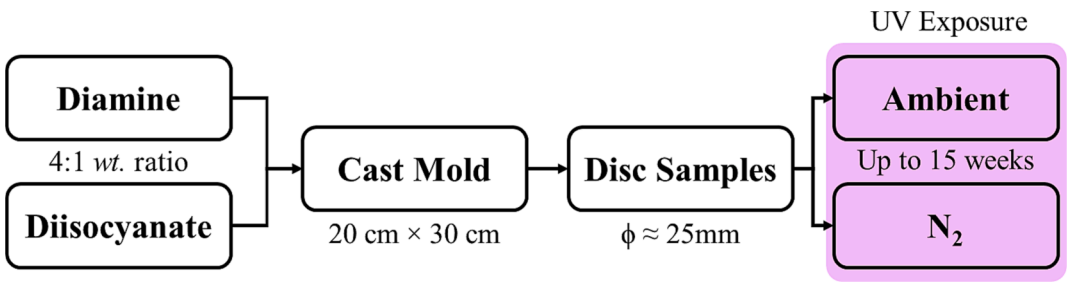

Fig. 1. Sample preparation and ultraviolet exposure processes.

2.2.1. Fourier transform Infrared spectroscopy (FTIR)

Regardless of the condition (*i.e.*, virgin, oxygen-rich, or N_2 atmosphere exposure), all samples were gently cleaned with methanol (67–56-1) at least 2 min before spectroscopic interrogation. Infrared spectra were collected using an FTIR-ATR (attenuated total reflectance) spectrometer (Thermo Scientific, Nicolet iS5 with the OMNIC software) with 32 scans and a linewidth resolution of 4 cm^{-1}. The samples were scanned in the spectral region of 400 cm^{-1} to 4000 cm^{-1}, capturing the fingerprint and functional group regions of aromatic polyurea. The peaks associated with amine and carbonyl groups are of specific interest to this study to explore the effect of extended ultraviolet radiation on monodentate and bidentate hydrogen bonding.

2.2.2. Terahertz time-domain spectroscopy (THz-TDS)

THz-TDS in transmission mode was used to probe the effect of ultraviolet radiation on the chemical structure of polyurea in the far-infrared region up to 1.7 THz. Since THz-TDS is less ubiquitous than FTIR-ATR, a brief introduction to this setup is included while referring the reader to [33,34] for a comprehensive review. Fig. 2a is a schematic representation of the built-in-house transmission THz-TDS setup used in this research, starting with a femtosecond laser (Menlo Systems, ELMO 780 HP) split into two optical paths. The first optical beam is focused on the active area of a photoconductive antenna (Tx, PCA, Batop, PCA-40-05-10-800) biased with a 40 V square wave pulse train, transmitting terahertz waves. The transmitted THz beam was collimated on the polyurea samples before being collected and focused onto the receiver photoconductive antenna (Rx, Batop, bPCA-100-05-10-800). The second optical beam was optically delayed, activating the receiving antenna simultaneously when the THz waves arrived at the receiver PCA. The converted and amplified signal as a measurable photocurrent was collected using a lock-in amplifier (Stanford Research Systems, SR830). It is imperative to mention that the THz waves have an affinity for airborne moisture, affecting the obtained spectra. Therefore, the terahertz beam path was placed inside an acrylic enclosure to control the moisture content within the scanning environment using desiccants (Drierite 8 mesh). To avoid reintroducing ambient humidity during sample exchange, five samples were concurrently mounted on an externally actuated rotating wheel with six 25 mm diameter slots, shown in Fig. 2b, leaving one unoccupied slot for reference measurements. The resulting time-domain signals (*i.e.*, terahertz amplitude-time histories) were analyzed using the Li *et al.* method [35] to extract the complex refractive index and the frequency domain for spectral analyses.

2.2.3. UV–visible absorption and excitation-emission matrix spectroscopy (EEMS)

UV–visible absorption and fluorescence spectra were recorded for all polyurea samples using a Duetta spectrometer controlled via the manufacturer's EzSpec software (Horiba). The Absorption spectra were scanned from 250 nm to 1000 nm in step increments of 1 nm. The fluorescence spectra were recorded using the excitation-emission matrix spectroscopy (EEMS) mode, in which fluorescence spectra were obtained for a series of excitation wavelengths, with each fluorescence spectrum normalized by the instrumental sensitivity correction factors and the absorbance value at the excitation wavelength. Excitation-emission matrices were obtained in the excitation and emission range of 400 nm to 800 nm at increments of 5 nm. Notably, the spectrum for each sample was obtained after acquiring a sample-free background spectrum.

3. Results and discussion

3.1. Fourier transform infrared spectroscopy (FTIR)

Fig. 3 shows the FTIR spectra collected from virgin and UV-exposed (irrespective of the atmospheric conditions) polyurea specimens over 400 cm^{-1} to 4000 cm^{-1}. The observed peaks are characteristic of polyurea [18], primarily attributed to the amine and carbonyl groups and the associated hydrogen bonds. The peaks at 1020–1100 cm^{-1} refer to the ether functional group, where attenuation in the absorption peak indicates cleavage. The absorption peaks in the 1600 cm^{-1} to 1700 cm^{-1} region correlate with the stretching vibrations of the carbonyl group, which broadened as a function of ultraviolet exposure, indicating possible scission of C = O bonds. A pertinent reduction in intensity in the stretching vibration of the C–H bond (at 2860–2970 cm^{-1}) implies potential disassociation as a function of exposure duration under ambient conditions. Similarly, the stretching vibration of the N–H bond at 3284–3287 cm^{-1} is affected by ultraviolet radiation, giving rise to structural changes attributed to hydrogen bonding. The structural changes in N–H bonds, exemplified as redshifting in this spectral region, further suggest bond cleavage, affecting the hydrogen bonding due to electronegativity differences. That is, ultraviolet-exposed polyurea is cardinally governed by the degree and state of hydrogen bonding,

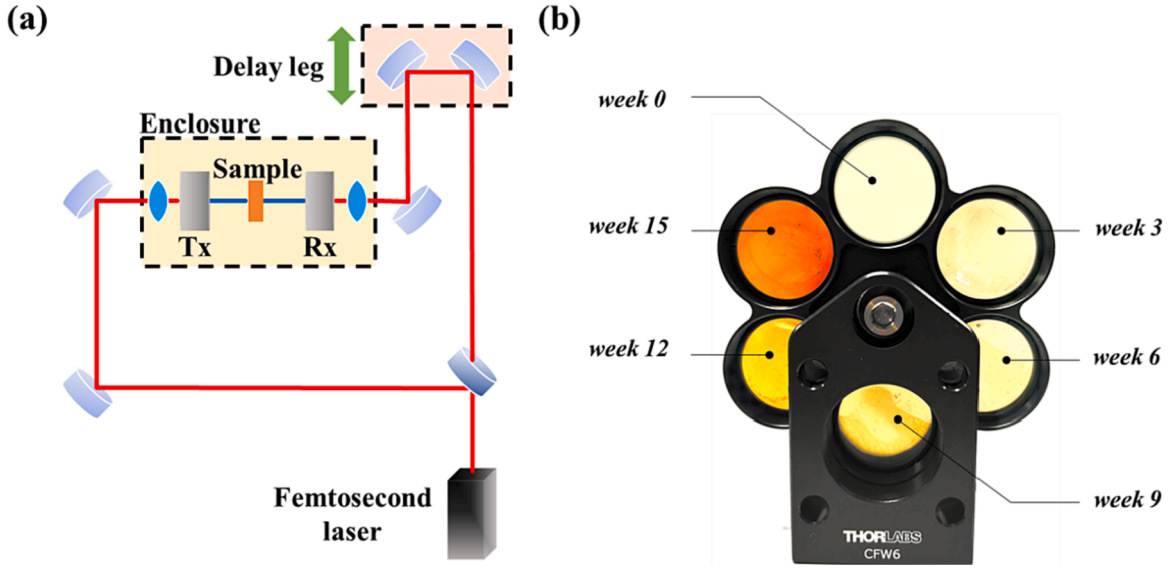

Fig. 2. (a) Schematic of the transmission terahertz time-domain spectroscopy (THz-TDS) used to probe the conformational changes in aromatic polyurea after extended ultraviolet exposure, and (b) polyurea samples in an externally actuated rotating wheel.

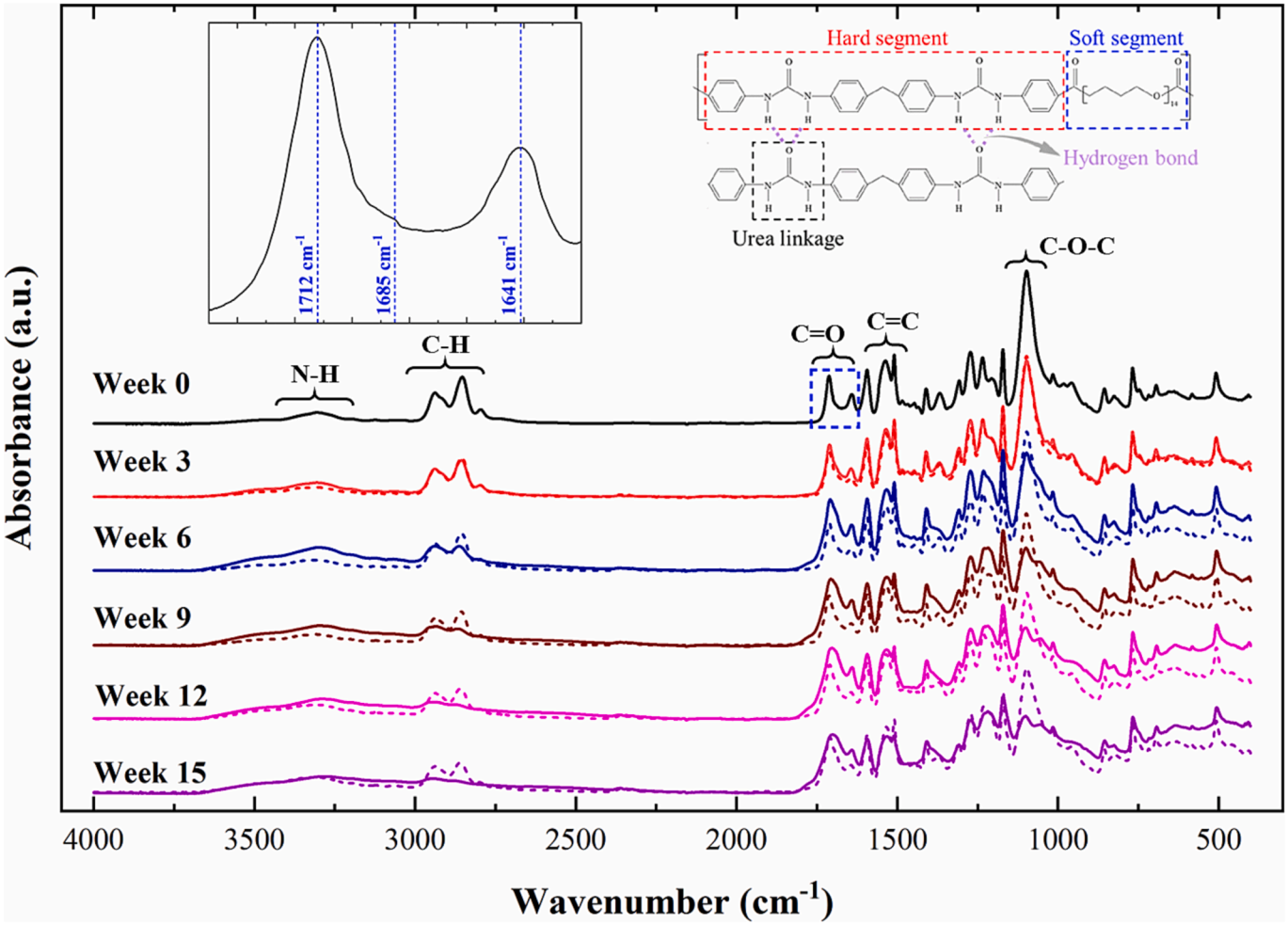

Fig. 3. FTIR-ATR absorption spectra of virgin and UV-radaited (ambient, *solid lines*, and nitrogen, *dotted lines*, atomspheres) aromatic polyurea samples as a function of exposure duration up to 15 weeks. The spectra highlight the UV effects on primary chemical groups.

significantly influenced by the N–H bond in the urea bond and the carbonyl (C = O) group, as discussed next.

The peaks observed at 1641 cm^{-1}, 1685 cm^{-1}, and 1712 cm^{-1} correspond to the ordered, disordered hydrogen-bonded, and hydrogen bond free urea carbonyls, respectively. The deconvolution of these peaks dilineates their respective intensities, faciliating the disucssion about the correlation between hydrogen bonding and ultraviolet exposure duration. The degree and state of hydrogen bonding can be calculated using

$$X_o = \frac{A_o}{(A_o + A_{dis} + A_{free})} \tag{1a}$$

$$X_{dis} = \frac{A_{dis}}{(A_o + A_{dis} + A_{free})} \tag{1b}$$

$$X_{free} = 1 - (X_o + X_{dis}) \tag{1c}$$

where, X_o, X_{dis}, and X_{free} denote the fraction of carbonyl groups having ordered, disordered, and no hydrogen bonds. A_o, A_{dis}, and A_{free} denote the area corresponding to respective peaks obtained after deconvolution [13,36]. Fig. 4 summarizes the results from analyzing the prominence of different hydrogen bonding based on Eqns. 1 for the ambient atmosphere (Fig. 4a) and nitrogen atmosphere (Fig. 4b).

Exposure to UV radiation in an ambient environment monotonically increases the degree of disordered hydrogen bonding (Fig. 4a) as a function of exposure duration, i.e., quasi-linearly ascending from the lowest level for virgin polyurea to the highest level after 15 weeks. The calculated percentage of disordered hydrogen bonding increased from 8 % for unexposed samples to 49.5 % at the end of the weathering period. The ordered and free hydrogen bonding exhibit a descending trend, decreasing from 30.5 % and 61.5 % for pristine samples to 19.3 % and 31.2 % after extended artificial weathering under ultraviolet radiation for 15 weeks, respectively. On the other hand, the percentage of disordered H-bond in the samples irradiated in the nitrogen atmosphere (Fig. 4b) shows a steep increase after three weeks of ultraviolet exposure, followed by a plateau as the exposure duration commenced. Correspondingly, the ordered H-bond decreased within the first three weeks of ultraviolet radiation, remaining nearly constant thereafter. Notably, the percentage of ordered H-bond within the polyurea structure remained nearly unchanged, ca. 18.7 %, irrespective of irradiation atmosphere, which could be linked to the limited effects of extended ultraviolet weathering on the mechanical properties of polyurea, as reported previously in [7–11,14]. The difference in the structural changes under the N_2 atmosphere compared to the ambient counterpart is attributed to the absorption of the former within the ultraviolet region, slowing the physical aging process. Artificial weathering in an ultraviolet environment generally affects segmental mobility, decreasing the free volume and altering the physical and mechanical properties [37,38]. Additionally, the FTIR spectra in Fig. 3 reveal shifting in the amino group towards low wavenumber, from 3308 cm^{-1} to 3281 cm^{-1}, for samples exposed under ambient atmosphere. This shifting is associated with the stretching vibrations of the N–H bonds and implies a reduction in the vibrational frequency, ω, ($\omega = \sqrt{k/m}$, where k is the

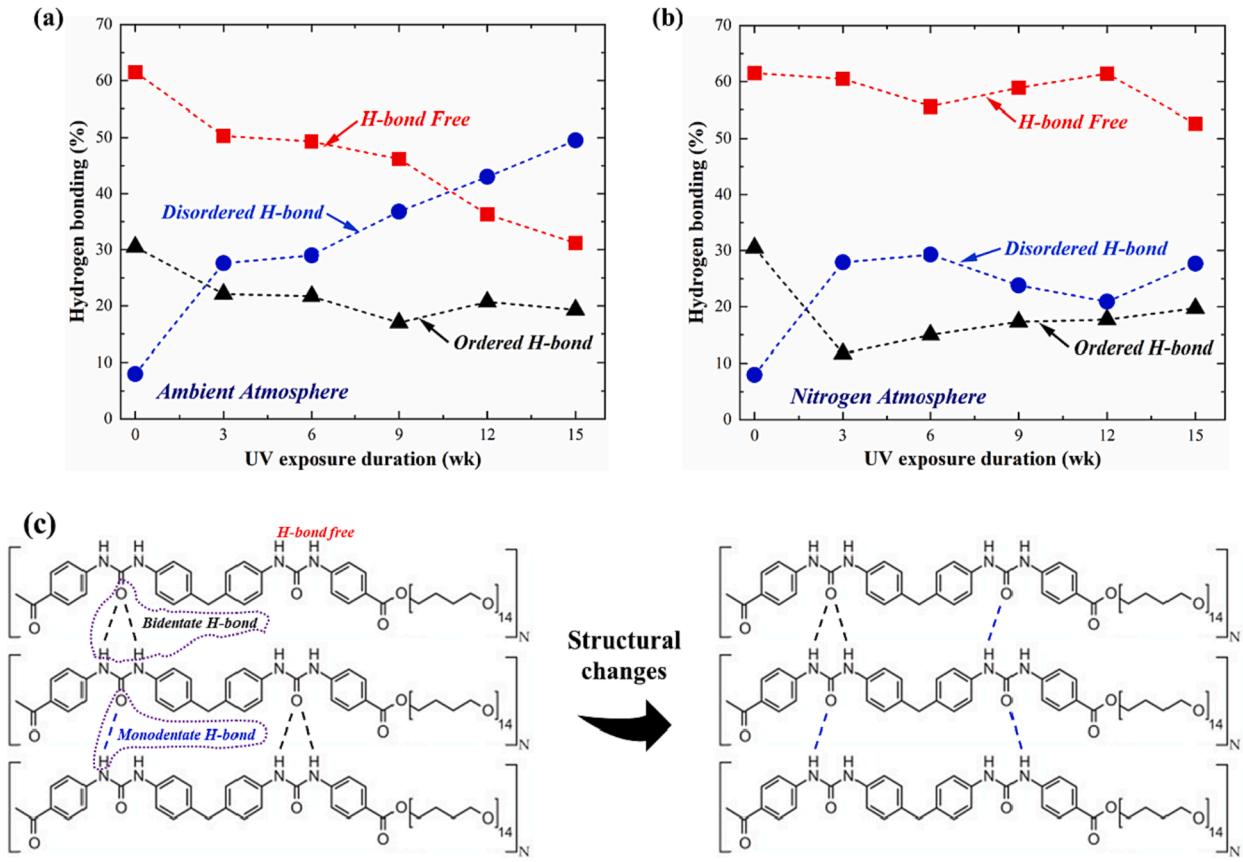

Fig. 4. Spectral deconvolution analyses within the carbonyl peaks reveal the interrelationship between hydrogen bonding in aromatic polyurea and ultraviolet exposure duration in (a) ambient and (b) nitrogen atmospheres. (c) Suggested macromeolcular structural changes due to monodentate and bidentate hydrogen bonding after ultraviolet exposure.

bond stiffness and m is the molecular mass). The shift towards lower wavenumber may be attributed to the increase in the total fraction of H-bonds (disordered and ordered) with increasing UV radiation exposure, weakening the stiffness of N–H bonds and decreasing the vibrational frequency or wavenumber as observed in the spectra.

Interestingly, the results in Fig. 4 show a positive correlation between the fraction of the disordered H-bonds and exposure duration, especially in samples irradiated under an ambient atmosphere. Based on the preceding discussion, Fig. 4c included probable structural changes to aromatic polyurea after extended ultraviolet radiation. These macromolecular changes necessitate future reactive molecular dynamic investigations to delve into the details leading to them. The increase in monodentate H-bonds is likely attributed to the decrease in free volume, enhancing chain affinity conducive to hydrogen bond formation and affecting the mechanisms responsible for the mechanical behavior of polyurea after ultraviolet irradiation [7]. The enhanced chain affinity also facilitates the intermolecular interaction between the hard segments, further increasing H-bond formation [39]. On the other hand, the bidentate H-bond fraction remains constant, which is associated with the energy required for bond formation. The stronger bidentate H-bond (21.8 kJ/mol) is higher than the weaker monodentate H-bond (18.4 kJ/mol) [40,41].

Finally, a key structural feature from the FTIR spectra is the length of the H-bond in amino groups. The peak at 3480 cm^{-1} is attributed to the amino groups without hydrogen bonds, while the peaks in the 3281 cm^{-1} to 3308 cm^{-1} range have been attributed to amino groups with hydrogen bonds. This shift provides an estimation of the hydrogen bond length based on [42]

$$R = 3.21 - \frac{\Delta V}{548} \quad (2)$$

where, ΔV signifies the horizontal shift in the wavenumber (difference between wavenumbers corresponding to amino groups with and without H-bonds), and R denotes the bond length (\AA). The resulting changes in the bond length as a function of exposure duration in ambient and nitrogen atmospheres are plotted in Fig. 5, exemplifying the significant effect of the surrounding atmosphere on the hydrogen bonding

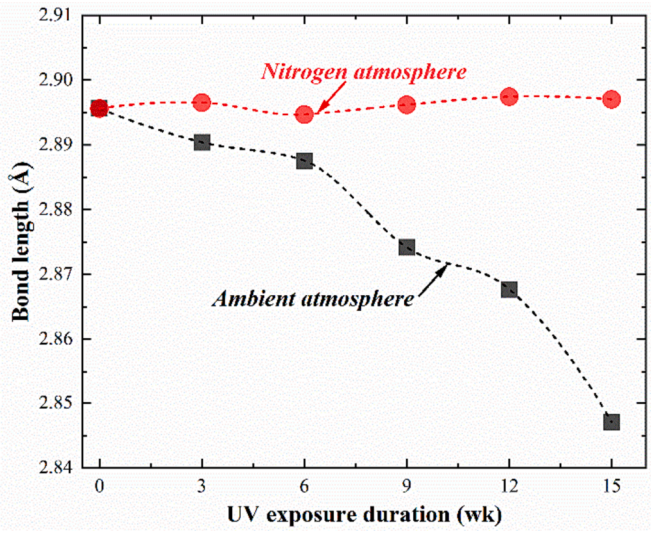

Fig. 5. Change in hydrogen bond length between amino and carbonyl groups in aromatic polyurea as a function of ultraviolet exposure duration and surrounding environment.

associated with the characteristic amino group within the aromatic polyurea structure. Hydrogen bond length decreases from 2.89 Å to 2.84 Å in unexposed and 15-week irradiated polyurea samples in the ambient atmosphere, respectively, due to the decrease in the free volume associated with bringing the amino group closer to one another. On the other hand, the change in the hydrogen bond length within this spectral peak in the nitrogen atmosphere remained nearly unchanged over the entire ultraviolet exposure duration since the surrounding N_2-rich environment shielded the polyurea macromolecule from photo-degradation and photo-oxidation processes reported before for the ambient counterpart [10].

3.2. Terahertz time-domain spectroscopy (THz-TDS)

Fig. 6 shows the experimental terahertz spectra collected from pristine and ultraviolet-exposed polyurea samples under ambient and nitrogen atmospheres. The time-domain signals from the samples and sample-free background scans were transformed to the frequency domain using the standard apodization technique commonly used in spectroscopic analyses [43]. The spectra in Fig. 6 are also annotated with experimental spectroscopic features at 0.69, 1.08, 1.27, 1.47, and 1.64 THz, previously reported by Zhao *et al.* for crystalline urea molecules (powdered form) [44]. Furthermore, Zhao *et al.* performed density functional theory (DFT) calculations, assigning molecular motions at 0.66 and 1.06 THz to inter urea-linkage hydrogen bonds [44], which was later probed experimentally by Hyunh *et al.* when investigating the shock effects on aromatic polyurea [45,46]. Some spectral features in the experimental spectra reported herein coincide with prior research while revealing additional peaks. Five spectral peaks are highlighted in Fig. 6, including ~ 1.13, 1.19, 1.24, 1.45, and 1.64 THz, denoted by dotted blue lines at the corresponding frequencies. These peaks are characteristically associated with the aromatic polyurea structure investigated herein [44]. Of specific note is the spectral feature at 1.64 THz detected in the current study, irrespective of the irradiation conditions and the study by Zhao *et al.* [44]. Notably, the prominence of the spectral feature located at 1.64 THz, showing a strong intensity, has also been experimentally and computationally confirmed by Zhao *et al.* when studying crystalline urea. An expanded discussion about the 1.64 THz peak is included in the forthcoming section. In general, the spectral features within this terahertz regime are associated with intermolecular vibrational modes, giving rise to the contributions of hydrogen bonding with the aromatic polyurea structure. The difference between the current results and the previous experimental and computational data is attributed to (1) the effects of the sample preparation process on the molecular structure of polymers, (2) the force fields used in DFT calculations, and (3) the spectral differences in the experimental setups (*e.g.*, laser pump, terahertz polarization, etc.).

The spectra in Fig. 6 reveal three additional overarching experimental observations as a function of the exposure atmospheres. First, the terahertz spectra measured from ultraviolet-exposed samples under a nitrogen atmosphere resemble the major attributes of the spectrum from the control, unexposed counterparts, as previously elucidated from the FTIR-ATR analysis. The persistence of the spectral peaks is apodictic despite the changes in prominence, associated with slight photo-degradation effects reported before due to the interactions between the ultraviolet radiation and the chromophore groups within the polyurea structure, even within the attenuative nitrogen atmosphere (*i.e.*, the tendency of the nitrogen to absorb the UV radiation). Second, the manifestation of additional peaks in aromatic polyurea, compared to the crystalline version reported previously by Zhao *et al.*, persisted irrespective of the exposure atmosphere, pointing to additional intermolecular vibrational features associated with monodentate and bidentate hydrogen bonding within the aromatic polyurea structure. This second observation is consistent with the segmented microstructure of polyurea

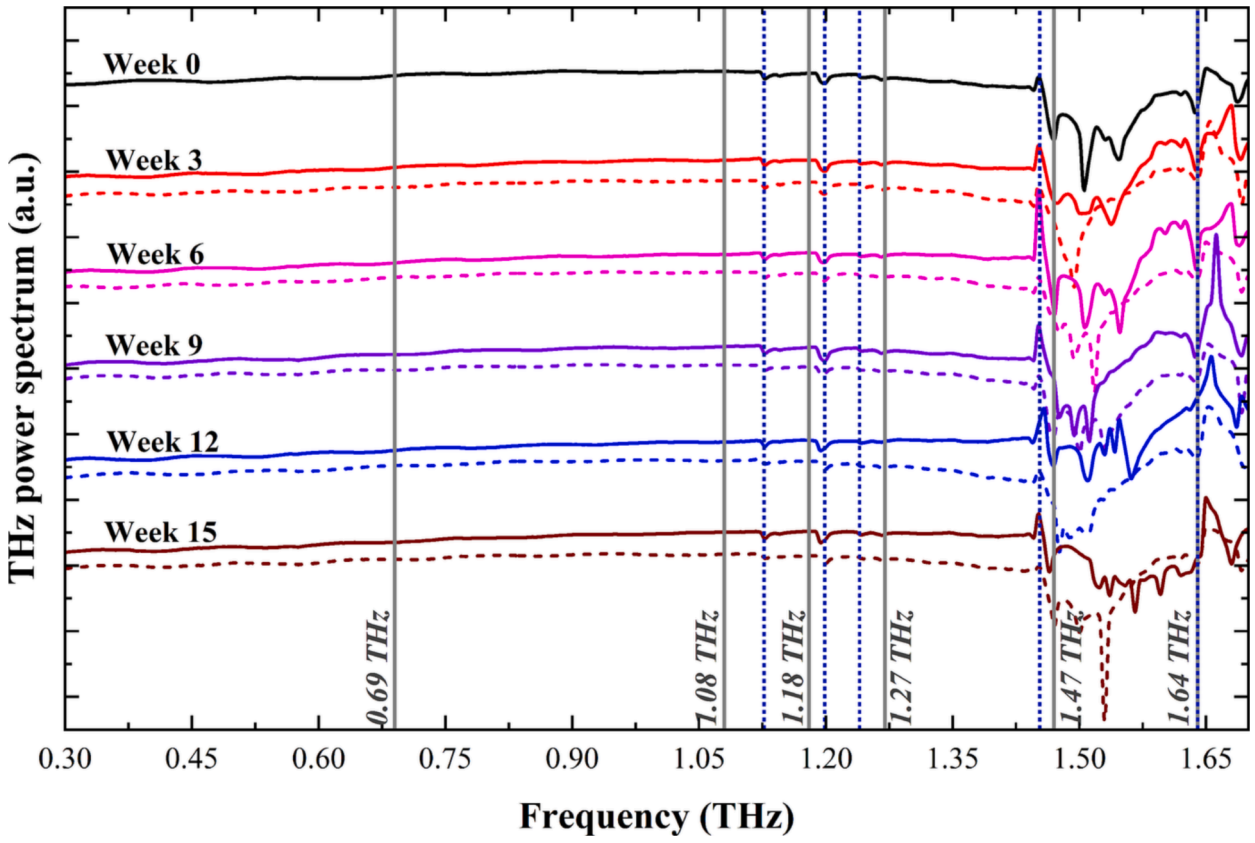

Fig. 6. Terahertz spectra of ultraviolet-irradiated polyurea samples under ambient (solid lines) and nitrogen (dotted lines) atmospheres for up to 15 weeks of continuous exposure compared to the spectral features of virgin counterparts.

consisting of hard (ordered) and soft (amorphous) domains stemming from the thermodynamic non-equilibrium during the step polymerization process.

Finally, the spectral peak at 1.64 THz elucidates an intriguing evolution as a function of exposure duration, evident in the spectra collected from samples weathered under ambient conditions. Specifically, the strong prominence of the peak at 1.64 THz continues to attenuate as the exposure duration increases while shifting the vibrational energy to the adjacent peak at 1.66 THz. This region in the terahertz regime was previously associated with the torsional vibration mode within the crystalline urea molecules, suggesting significant contributions to the intermolecular hydrogen bonds in polyurea [44]. The latter was initially subdued but dominated this spectral region at the end of the exposure duration, *i.e.*, after 15 weeks of continuous exposure. Future research by this group is focused on composing molecular mechanics and dynamic simulations of aromatic polyurea macromolecules to overcome the current challenges in interpreting the experimental terahertz spectrum while exploring the spectral contributions of hydrogen bonding within this strategic material system.

Fig. 7 is a composite plot of the refractive indices and absorption coefficients extracted from the terahertz time-domain signals using the extraction method by Li *et al.* based on fitting the signals into the transfer function [35]. For each testing condition (*i.e.*, exposure atmosphere, duration, etc.), the reference (sample-free) and sample time-domain signals and the sample mechanical thickness (measured using an ultrasound probe, Positector 6000) were fed into the algorithm to extract the optical indices in terms of the real refractive index and the absorption coefficient. The method of Li *et al.* hinges on initially transforming the time-domain signals into the frequency domain using discrete Fourier transform, fitting the transformed data into a theoretical transfer function that encompasses the effects of the complex refractive index and the Fabry-Pérot oscillations, and transforming the optimized fit back into the time-domain for correlation check with the original terahertz time-domain signals. Irrespective of the exposure duration and atmosphere, the refractive indices elucidate three experimental observations.

First, the spectra features reported above, *i.e.*, absorption peaks, persisted despite the difference in the analysis approach, confirming the molecular origin of these spectral peaks. For example, the spectral peaks at 1.10, 1.17, 1.42, 1.61, and 1.67 THz are ubiquitous in plots in Fig. 7, regardless of the exposure duration and atmosphere. The manifestation of these spectral peaks is a testament to the reliability of the optical properties extraction algorithm, where others obscured these spectroscopic features due to over-filtering and smoothing [35]. Second, the values of the real refractive index and absorption coefficient for virgin polyurea are found to be in good agreement with previous results reported in [47]. Finally, the effects of exposure under the N_2 atmosphere on the complex index as a function of exposure duration is minimal, further asserting the observations based on FTIR-ATR in § 3.1. The

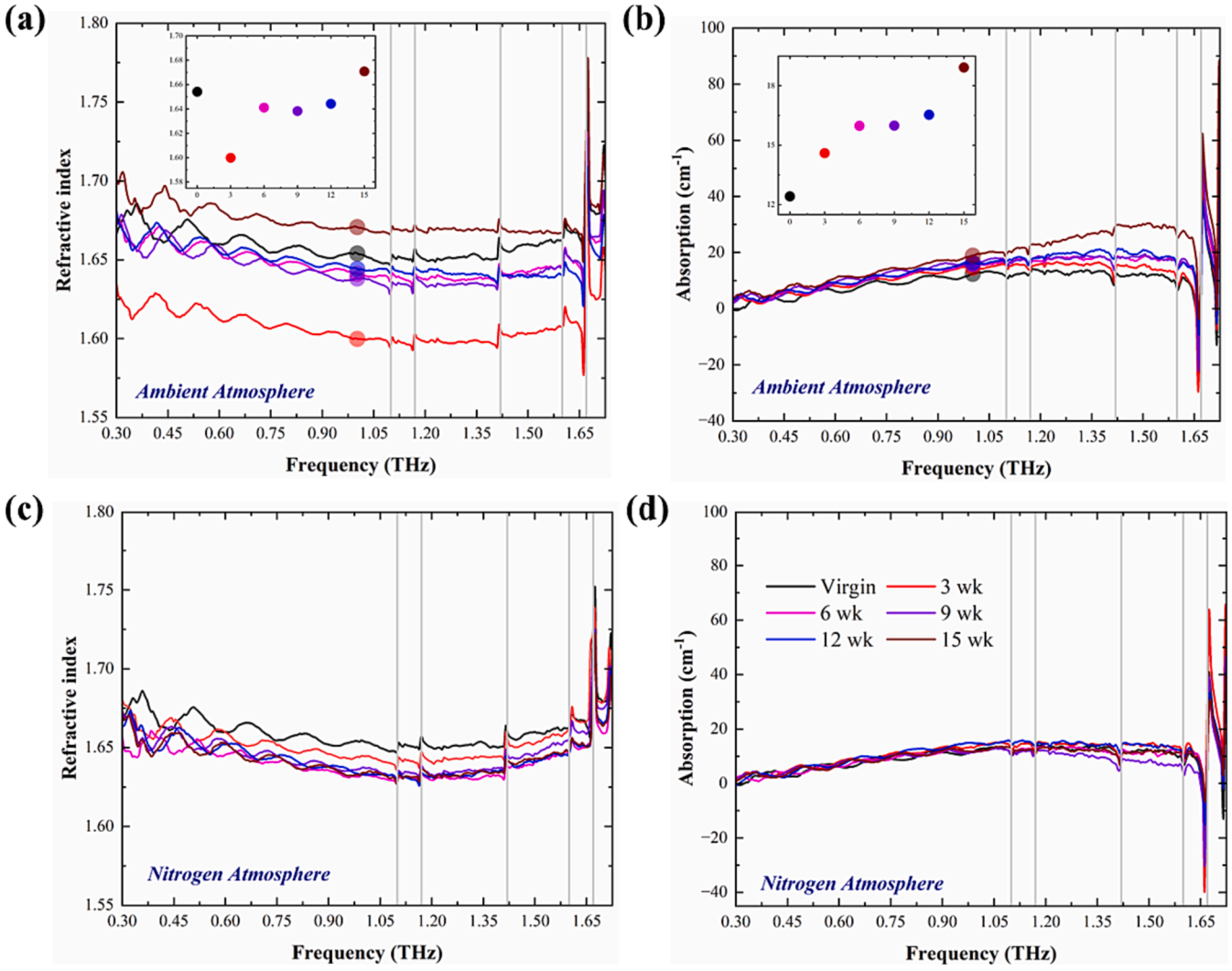

Fig. 7. Refractive index and absorption spectrum of virgin and UV-exposed polyurea samples irradiated in (a, b) ambient atmosphere (c, d) N_2 atmosphere, respectively (Inset shows the index and absorption values for virgin and exposed samples as a function of UV exposure duration at a frequency of 1 THz).

values of the refractive index and the absorption coefficient as a function of frequency remained nearly bundled around the indices extracted from the virgin counterparts despite extended exposure under nitrogen atmospheres for up to 15 weeks. However, exposure under an ambient atmosphere resulted in notable differences in the refractive indices as a function of the exposure duration while considering the differences in the mechanical thickness of each sample.

On the one hand, the slight difference in the index spectra in Fig. 7c and 7d for the refractive and absorption coefficients, respectively, due to the ultraviolet exposure of aromatic polyurea under nitrogen atmospheres are generally attributed to the limited photodegradation mechanisms. The latter is accompanied by apparent discoloration (*e.g.*, Fig. 2b) due to the superiority of the photonic energy within the unshielded ultraviolet radiation to the activation energy of aromatic polyurea [48]. On the other hand, the refractive and absorption coefficients of the polyurea samples exposed in the ambient atmosphere show dependence on the exposure duration. The refractive index decreased due to increasing exposure duration when polyurea samples were irradiated with ultraviolet light under an ambient atmosphere. The inset in Fig. 7a collates the refractive index values related to the exposure duration, ranging from 1.65 for the control samples to 1.67 after extended exposure for 15 weeks. The absorption coefficient increased as a function of exposure duration, ranging from 12.41 cm^{-1} for the virgin samples to 18.92 cm^{-1} for UV-exposed samples for 15 weeks under an ambient atmosphere, extracted at 1 THz. The inset in Fig. 7b summarizes the absorption coefficient values as a function of exposure duration at 1 THz, elucidating the monotonically increasing trend. Since the ambient atmosphere comprises oxygen and moisture, the changes in the complex refractive index are attributed to photodegradation and photooxidation mechanisms, resulting in discoloration, surface crazing, and agglomeration of the hard domains [7].

3.3. Emission-Excitation matrix spectroscopy (EEMS)

The excitation-emission spectra for polyurea samples subjected to UV radiation are shown in Fig. 8. The virgin samples exhibit a faint emission in the visible region at a wavelength of 50 nm higher than the excitation wavelength, the intensity of which becomes feeble for 3-week samples before disappearing for 6-week exposed samples. The emission at excitation wavelength depicts the fluorescence characteristics of polyurea, which may be attributed to the cluster formation of the molecular chains in accordance with the cluster-triggered-emission mechanism, usually observed in compounds with the absence of traditional chromophores [49,50]. In these clusters, the electron clouds of these unconventional groups overlap, reducing the energy gap and facilitating the fluorescence. In polymers with functional groups composed of heteroatoms (*e.g.*, nitrogen or oxygen), such as polyurea due to electron-rich urea, clusters are formed by aggregation of the heteroatoms on polymer chains. Polyurea is comprised of the phenyl ring and the urea group. However, the former is considered a traditional chromophore with emission in the UV region, in contrast to the emission observed here in the visible region [51]. The manifestation of a secondary peak in virgin samples at 50 nm higher than the excitation wavelength suggests Raman emission. However, the intensity of the secondary peak is significantly suppressed after 3-week UV exposure before being diminished for 6-week exposed samples, attributed to the self-absorption behavior of UV-radiated polyurea samples. Interestingly, the intensity of the secondary peak becomes prominent again for 9-week and 12-week exposed samples. The extended exposure to UV radiation initially facilitates the self-absorption of the samples irradiated continuously under ambient atmosphere for 3 and 6 weeks, followed by significant fluorescence in those irradiated for 9 and 12 weeks.

Furthermore, the Raman emission in the latter is subdued at higher excitation wavelengths, prompting the wavelength-dependent self-absorption behavior and the duration of UV exposure. The latter can be attributed to the excitation-dependent emission, *i.e.*, the emission strongly dependent on the excitation wavelength, especially in the visible region for non-chromophore molecules. The intensity of emission is dependent on the size of the formed clusters, which may be attributed to the agglomeration of the hard domains with phenyl rings inherited from the polycarbodiimide-modified diphenylmethane diisocyanate, as reported before in [7]. Notably, the coexistence of the urea group, as discussed above, is imperative for self-absorption to be detectable. The increase in the agglomeration rate of the hard segments was previously reported by Blourchian *et al.* to be 0.67 %/wk up to 6 weeks of exposure, ascending to 1 %/wk after that, reaching nearly 90 % surface coverage

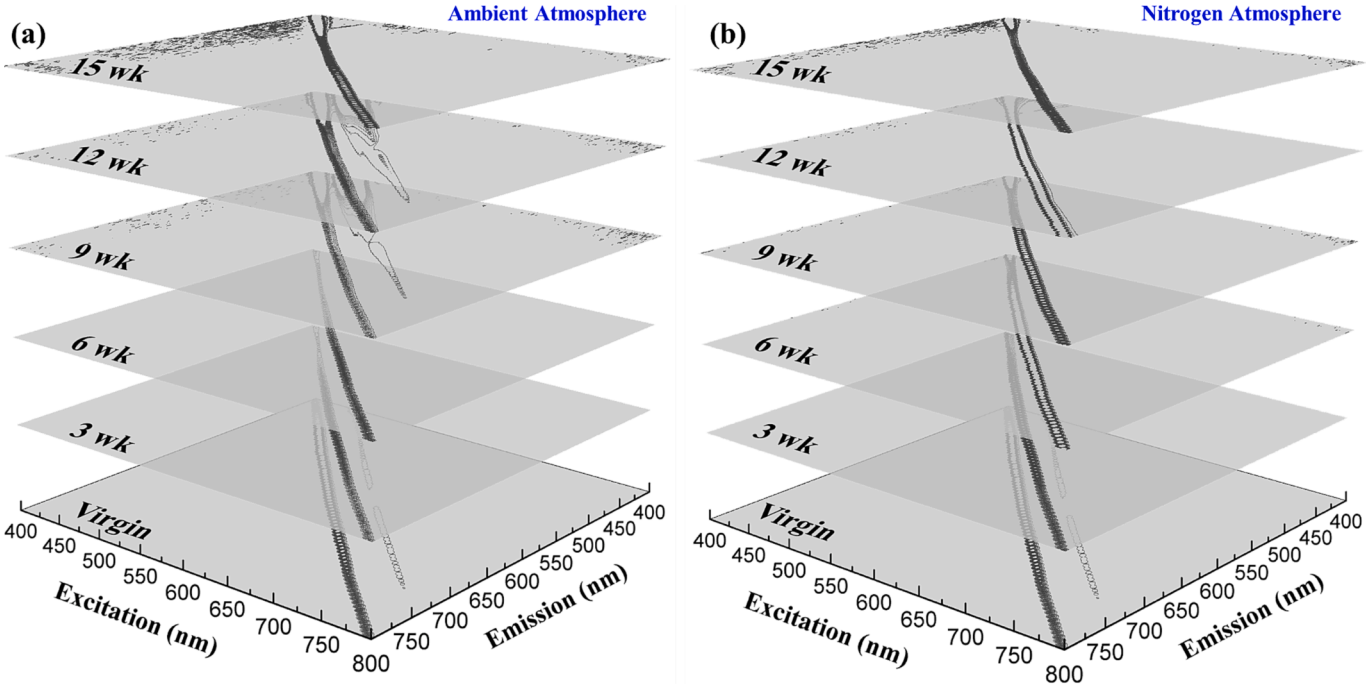

Fig. 8. Excitation emission matrix spectra of polyurea samples subjected to UV radiation under (a) ambient and (b) nitrogen atmospheres.

after 15 weeks of continuous ultraviolet radiation. Such an increase in hard domain coverages obscures access of the excitation wavelength to the urea group under the surface. Remarkably, the fluorescence was not detectable in 15-week samples, affirming the hypothesis regarding the coexistence of the phenyl and urea groups and the effect of hard segment agglomeration on the emission attributes. These observations are also consistent with an earlier report on pure oxygenic nonconjugated poly (maleic anhydride-alt-vinyl acetate) by Tang *et al.*, which revealed the formation of a heterodox cluster of carbonyl groups when subjected to UV radiation [50]. The EEM spectra of samples irradiated under nitrogen atmospheres expectedly exhibited fluorescence but no self-absorption, as shown in Fig. 8b. This can be attributed to the slowing down of degradation in a nitrogen atmosphere and thus prevents the exposure levels required for the re-manifestation of the Raman emission.

Fig. 9 shows the absorption spectra of the polyurea samples subjected to UV radiation under ambient (solid lines) and nitrogen (dotted lines) atmospheres. The absorption of irradiated polyurea samples in the ambient atmosphere dominates their nitrogen environment counterparts, irrespective of the exposure duration. For example, the absorption at 600 nm is 0.136, 0.275, and 0.2 for virgin and 9-week irradiated samples in ambient and N_2 atmospheres, respectively. Similar differences are reported for the remaining exposure durations comparatively. In general, the absorption affinity shows a monotonic increase with respect to the exposure duration. Nonetheless, the increase in ultraviolet exposure duration is associated with a shifting of the absorption range within the visible regime, while the absorption of the virgin polyurea occurs almost entirely in the UV regime. The monotonic absorption enhancement can be correlated to the color change upon radiation, darkening from light yellow for unexposed samples to dark tan after 15 weeks of continuous exposure. Notably, the variation across various exposure time frames is non-uniform, where initial UV exposure leads to higher absorbance, but it saturates upon further higher radiation duration.

4. Conclusion

The research aims to probe the effect of continuous exposure to UV radiation on the conformational characteristics of aromatic polyurea elastomers by employing various spectroscopic techniques. Polyurea samples irradiated with ultraviolet rays for up to 15 weeks under ambient and nitrogen atmosphere were investigated using FTIR-ATR spectroscopy to elucidate the effect of extended radiation on the molecular structure. A significant monotonic increase in the degree of disordered H-bond was observed in the case of ambient-irradiated samples compared with samples irradiated under a nitrogen atmosphere. In addition to the degree of bonding, the H-bond length was found to exhibit a variation of 0.05 \AA in the former, as compared to a marginal variation in the latter. THz-TDS characterization revealed a similar inference with the ambient samples, exhibiting a high variation in refractive index and absorption coefficient as compared to the nitrogen-irradiated samples. Furthermore, EEMS was employed to discern the effect of UV radiation on fluorescence characteristics of UV-irradiated polyurea, where 9-week and 12-week samples reported significant self-fluorescence that was attributed to the cluster triggered emission. This research not only provides a comprehensive understanding of the behavior of UV-exposed polyurea elastomers but also unlocks new research avenues, such as detailed further investigation of the underpinnings associated with the observed fluorescence behavior.

CRediT authorship contribution statement

Amritesh Kumar: Formal analysis, Data curation, Investigation, Methodology, Writing – review & editing, Writing – original draft. **David Pullman:** Data curation, Methodology, Resources, Writing – original draft. **George Youssef:** Conceptualization, Data curation, Formal analysis, Funding acquisition, Methodology, Project administration, Visualization, Writing – review & editing, Writing – original draft.

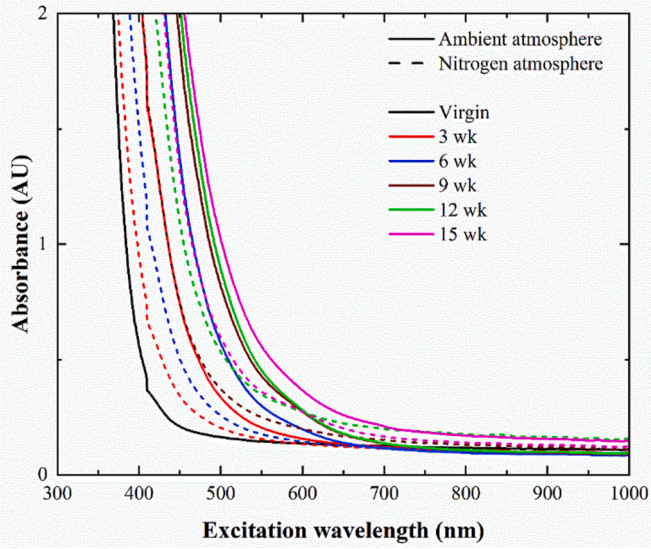

Fig. 9. Absorption spectra of virgin and UV-exposed polyurea samples radiated under ambient (solid lines) and nitrogen (dashed lines) atmosphere.

Declaration of competing interest

The authors declare that they have no known competing financial interests or personal relationships that could have appeared to influence the work reported in this paper.

Data availability

Data will be made available on request.

Acknowledgment

The research leading to these results was supported in part by the United States Department of Defense under Grant Agreement No. W911NF1410039 and W911NF1810477. The National Science Foundation under Award No. 1925539 also supported the research. The authors are also grateful for internal funding from San Diego State University.

References

[1] R.G.S. Barsoum, *Elastomeric polymers with high rate sensitivity: applications in blast, shockwave, and penetration mechanics*, William Andrew, 2015.
[2] V. Gupta, et al., Adhesive and ultrahigh strain rate properties of polyurea under tension, tension/shear, and pressure/shear loadings with applications to multilayer armors, Elastomeric Polymers High Rate Sensitivity: Applications Blast, Shockwave, Penetration Mechanics 1 (2015) 71–92.
[3] N. Iqbal, et al., Polyurea coatings for enhanced blast-mitigation: a review, RSC Adv. 6 (111) (2016) 109706–109717.
[4] C. Angeloff, E.P. Squiller, K.E. Best, Two-component aliphatic polyurea coatings for high productivity applications, J. Protect. Coat. Linings(USA) 19 (8) (2002) 42–47.
[5] K. Palaniandy, et al., Formulations and properties: comparative review of aromatic polyurea vs aliphatic polyurea, Polyurea (2023) 3–15.
[6] F. John, V. Ray, The Use of UV Stabilizers in Aliphatic Polyurea Coatings, Polyurea Dev. Assoc. (2002).
[7] A. Blourchian, et al., Segmental evolution of ultraviolet weathered polyurea, J. Polym. Res. 28 (2021) 1–9.
[8] A.M. Shaik, N.U. Huynh, G. Youssef, Micromechanical behavior of ultraviolet-exposed polyurea, Mech. Mater. 140 (2020) 103244.
[9] G. Youssef, J. Brinson, I. Whitten, The effect of ultraviolet radiation on the hyperelastic behavior of polyurea, J. Polym. Environ. 26 (2018) 183–190.
[10] G. Youssef, I. Whitten, Dynamic properties of ultraviolet-exposed polyurea, Mech. Time-Dependent Mater. 21 (2017) 351–363.
[11] I. Whitten, G. Youssef, The effect of ultraviolet radiation on ultrasonic properties of polyurea, Polym. Degrad. Stab. 123 (2016) 88–93.

[12] C. Javier, et al., Effect of prolonged ultraviolet radiation exposure on the blast response of fiber reinforced composite plates, J. Mater. Eng. Perform. 28 (2019) 3174–3185.
[13] K. Che, et al., Investigations on aging behavior and mechanism of polyurea coating in marine atmosphere, Materials 12 (21) (2019) 3636.
[14] D.M. Pooria Pasbakhsh, K. Palaniandy, Sheik Ambarine Banon Auckloo, in: *Polyurea: Synthesis, Properties,* Composites, Production, and Applications, Elsevier, 2023, p. 430.
[15] R. Rinaldi, et al., Microstructure evolution during tensile loading histories of a polyurea, J Polym Sci B 49 (23) (2011) 1660–1671.
[16] I.N. Mforsoh, J. LeBlanc, A. Shukla, Constitutive compressive behavior of polyurea with exposure to aggressive marine environments, Polym. Test. 85 (2020) 106450.
[17] H. Kim, et al., Dynamic fracture energy of polyurea-bonded steel/E-glass composite joints, Mech. Mater. 45 (2012) 10–19.
[18] M. Tripathi, et al., Strain rate sensitivity of polyurea coatings: Viscous and elastic contributions, Polym. Test. 86 (2020) 106488.
[19] A. Sánchez-Ferrer, D. Rogez, P. Martinoty, Synthesis and characterization of new polyurea elastomers by sol/gel chemistry, Macromol. Chem. Phys. 211 (15) (2010) 1712–1721.
[20] R.F. Landel, L.E. Nielsen, Mechanical properties of polymers and composites, CRC Press, 1993.
[21] R. Hirt, N. Searle, R. Schmitt, Ultraviolet degradation of plastics and the use of protective ultraviolet absorbers, Polym. Eng. Sci. 1 (1) (1961) 21–25.
[22] L.M. Matuana, D.P. Kamdem, Accelerated ultraviolet weathering of PVC/wood-flour composites, Polym. Eng. Sci. 42 (8) (2002) 1657–1666.
[23] T. Turton, J. White, Effect of stabilizer and pigment on photo-degradation depth profiles in polypropylene, Polym. Degrad. Stab. 74 (3) (2001) 559–568.
[24] A. Hulme, N. Mills, The analysis of weathering tests on industrial helmets moulded from coloured polyethylene, Plast. Rubber Compos. Process. Appl. 22 (5) (1994) 285–303.
[25] C. Decker, K. Zahouily, Photodegradation and photooxidation of thermoset and UV-cured acrylate polymers, Polym. Degrad. Stab. 64 (2) (1999) 293–304.
[26] K.W. Ng, et al., Ultraviolet (UV) resistivity of polyurea composites, in: Polyurea, Elsevier, 2023, pp. 131–154.
[27] D.C.H. Chin, et al., High performance aliphatic polyurea films reinforced using nonfunctionalized multiwalled carbon nanotubes, Polym. Compos. 41 (3) (2020) 1036–1044.
[28] D. Cai, M. Song, High mechanical performance polyurea/organoclay nanocomposites, Compos. Sci. Technol. 103 (2014) 44–48.
[29] X. Qian, et al., Graphite oxide/polyurea and graphene/polyurea nanocomposites: a comparative investigation on properties reinforcements and mechanism, Compos. Sci. Technol. 74 (2013) 228–234.
[30] H. Wang, et al., A comparative study on UV degradation of organic coatings for concrete: Structure, adhesion, and protection performance, Prog. Org. Coat. 149 (2020) 105892.
[31] S. Do, et al., Thermomechanical investigations of polyurea microspheres, Polym. Bull. (2022) 1–15.
[32] J. Mattia, P. Painter, A Comparison of Hydrogen Bonding and Order in a Polyurethane and Poly (urethane− urea) and Their Blends with Poly (ethylene glycol), Macromolecules 40 (5) (2007) 1546–1554.
[33] R.M. Smith, M.A. Arnold, Terahertz time-domain spectroscopy of solid samples: principles, applications, and challenges, Appl. Spectrosc. Rev. 46 (8) (2011) 636–679.
[34] A. Rostami, H. Rasooli, H. Baghban, Terahertz technology: fundamentals and applications, Springer Science & Business Media, 2010.
[35] X. Li, et al., Precisely optical material parameter determination by time domain waveform rebuilding with THz time-domain spectroscopy, Opt. Commun. 283 (23) (2010) 4701–4706.
[36] J.G. Chavan, et al., Hydrogen bonding and thermomechanical properties of model polydimethylsiloxane based poly (urethane-urea) copolymers: Effect of hard segment content, Prog. Org. Coat. 90 (2016) 350–358.
[37] I.K. Meier, M. Langsam, H.C. Klotz, Selectivity enhancement via photooxidative surface modification of polyimide air separation membranes, J. Membr. Sci. 94 (1) (1994) 195–212.
[38] Q. Liu, et al., Effect of UV irradiation and physical aging on O2 and N2 transport properties of thin glassy poly (arylene ether ketone) copolymer films based on tetramethyl bisphenol A and 4, 4′-difluorobenzophenone, Polymer 87 (2016) 202–214.
[39] D. Ionita, et al., Tailoring the hard domain cohesiveness in polyurethanes by interplay between the functionality and the content of chain extender, RSC Adv. 5 (94) (2015) 76852–76861.
[40] J. Luo, et al., Mini-Review of Self-Healing Mechanism and Formulation Optimization of Polyurea Coating, Polymers 14 (14) (2022) 2808.
[41] M. Tahir, et al., Blending in situ polyurethane-urea with different kinds of rubber: performance and compatibility aspects, Materials 11 (11) (2018) 2175.
[42] P. Lu, G. Chen, W. Huang, Study on synthesis, morphology and properties of novel polyureas based on polyaspartic esters, J. Chem. Eng. Chin. Univ. 22 (1) (2008) 106.
[43] D.A. Naylor, M.K. Tahic, Apodizing functions for Fourier transform spectroscopy, JOSA A 24 (11) (2007) 3644–3648.
[44] Y. Zhao, et al., Intermolecular vibrational modes and H-bond interactions in crystalline urea investigated by terahertz spectroscopy and theoretical calculation, Spectrochim. Acta A Mol. Biomol. Spectrosc. 189 (2018) 528–534.
[45] N.U. Huynh, G. Youssef, In-operando spectroscopic interrogation of macromolecular conformational changes in polyurea elastomers under high strain rate loading, J. Mech. Phys. Solids 175 (2023) 105297.
[46] N.U. Huynh, C. Gamez, G. Youssef, Spectro-Microscopic Characterization of Elastomers Subjected to Laser-Induced Shock Waves, Macromol. Mater. Eng. 307 (2) (2022) 2100506.
[47] N.U. Huynh, G. Youssef, Ex situ spectroscopic characterization of residual effects of thermomechanical loading on polyurea, J. Eng. Mater. Technol. 144 (3) (2022) 031002.
[48] D. Fragiadakis, et al., Segmental dynamics of polyurea: Effect of stoichiometry, Polymer 51 (1) (2010) 178–184.
[49] E. Zhao, et al., Poly [(maleic anhydride)-alt-(vinyl acetate)]: A pure oxygenic nonconjugated macromolecule with strong light emission and solvatochromic effect, Macromolecules 48 (1) (2015) 64–71.
[50] W. Zhang Yuan, Y. Zhang, Nonconventional macromolecular luminogens with aggregation-induced emission characteristics, J. Polym. Sci. A Polym. Chem. 55 (4) (2017) 560–574.
[51] H. Cao, et al., Fluorescent linear polyurea based on toluene diisocyanate: Easy preparation, broad emission and potential applications, Chem. Eng. J. 399 (2020) 125867.